Evolution of surface to bulk tunneling spectrum by scanning tunneling microscopy

Y. C. Liao (廖延宗),[1] C. K. Yang (楊謹綱),[1] T. L. Wu (吳宗霖),[2] I. S. Hwang (黃英碩),[2] M. K. Wu (吳茂昆),[2] and C. C. Chi (齊正中)[1]

[1]*Department of Physics, National Tsing Hua University, Hsinchu, Taiwan, Republic of China*

[2]*Institute of Physics, Academia Sinica, Nankang, Taipei, Taiwan, Republic of China*

(Received 22 February 2010; revised manuscript received 12 April 2010; published 26 May 2010)

By decreasing tip-to-surface separation on the Si(111)−7×7 surface, we have observed symmetry change in topographic images and evolution from surfacelike to bulklike energy spectra. Because the tunneling is via Si adatoms interfacing to the bulk, the barrier heights at Si atoms of different dangling bonds are inhomogeneous. The observed phenomena can be numerically explained by a model of shifting chemical potential of the surface electrons due to the competing coupling strengths between the states of the tip, the surface, and the bulk. It leads to the conclusion that we have probed the interfacial coupling between electronic states of surface atoms and the bulk with atomic resolution.

DOI: 10.1103/PhysRevB.81.195435 PACS number(s): 73.20.At, 68.37.Ef, 73.25.+i, 73.40.Gk

I. INTRODUCTION

Since the invention of scanning tunneling microscopy (STM) by Binnig *et al.*,[1] it has become a prevailing tool to study surface states down to atomic scale.[2] Bulk states such as superconducting order parameter can also be measured using this technique.[3] However, it has not been used to explore the bulk-surface interface with atomic resolution. Early research on the bulk-surface interface typically focused on surface scattering at structures of impurity atoms[4] or monatomic step.[5] Studies of the intermediate layer between the surface and the bulk are relatively few. Some researchers have observed indirectly the effect of the magnetic exchange couplings of bulk electrons on surface states, which resulted in phenomena such as quantum mirage[4] and the magnetization of a single adatom.[6] To our knowledge, the use of ballistic-electron-emission microscopy[7] to resolve the subsurface Schottky barrier between a metal film and a semiconductor substrate with nanometer resolution is the only direct study of the interface. Because of increased interest in both theoretical and experimental studies of the conducting oxide interface,[8–10] the understanding of subsurfaces with atomic resolution becomes crucial. Our discovery of a new methodology to explore the interfacial coupling on Si(111)−7×7 might also be very useful for studying other materials in the future.

The distinctive surface layer of the 7×7 reconstruction naturally provides us with a perfect subsurface to study. According to the Dimer-Adatom-Stackingfault (DAS) model,[11] the surface [Fig. 1(a)] shows a different two-dimensional (2D) symmetry to that of unperturbed Si(111) plane. As indicated in a theoretical calculation,[12] this surface is of a metallic phase, but close to a metal-insulator transition. Its low conductivity[13] and the Si semiconducting gap make it easier to investigate the spectral evolution from surface states to bulk states probed by using scanning tunneling spectroscopy (STS).

In this paper, we present our studies on the tip-height dependence of topographic image, spectra of differential conductance, and tunneling currents. The idea is based on that decrease of the tip-surface separation reduces tunneling barrier between the STM tip and sample.[14–17] The evolution of density of states (DOS) from surface states to bulk states is measured as the tip approaches the sample surface. It is important that the surface-bulk interface remains pristine during the experiment. We describe experimental details in Sec. II. In Sec. III, the experimental data and analyses are presented. Based on the experimental observations, we develop a numerical model to explain the results, which is shown in Sec. IV. Finally, Sec. V contains a conclusion of this study.

II. EXPERIMENT

A three-chamber (loading chamber, sample preparation chamber, low-temperature chamber) UHV system is used for this study. The Si(111)−7×7 surface is prepared by repeatedly annealing a *p*-type Si(111) substrate (boron doped, resistivity of 0.05 to 0.1 Ω cm) in the UHV (about 1×10^{-10} torr) sample preparation chamber. The processed sample is then transferred to the STM stage at 4.3 K. We use a Pt-Ir tip to measure the STM and STS of the surface. The advantage of using this tip and *p*-type Si is the smaller contact potential, 0.15 eV, compared to the typical value of about 0.5 eV between a W tip and *n*-type Si. Our Pt-Ir tip is cleaned *in situ* by touching the surface gently and then is refined by repetitively scanning over Si steps. The sample bias is fixed at +2 V for taking topographic images and for measuring the tip-height dependence of tunneling currents $I(z)$. During image scanning, at some chosen sites, the scanning is halted and the feedback loop is opened and then the spectra of $I(v)$ and $I(z)$ are measured. This procedure ensures the spectra are measured at the specific atomic site. The relative tip displacement z is controlled by piezovoltage and is calibrated against a single atomic step on Si(111) surface. We obtain the spectra of differential conductance (dI/dV) by differentiating the *I*-*V* curves numerically.

III. RESULTS AND DISCUSSION

The first hint of detecting the subsurface is provided by a series of topographic images taken at different tip heights at

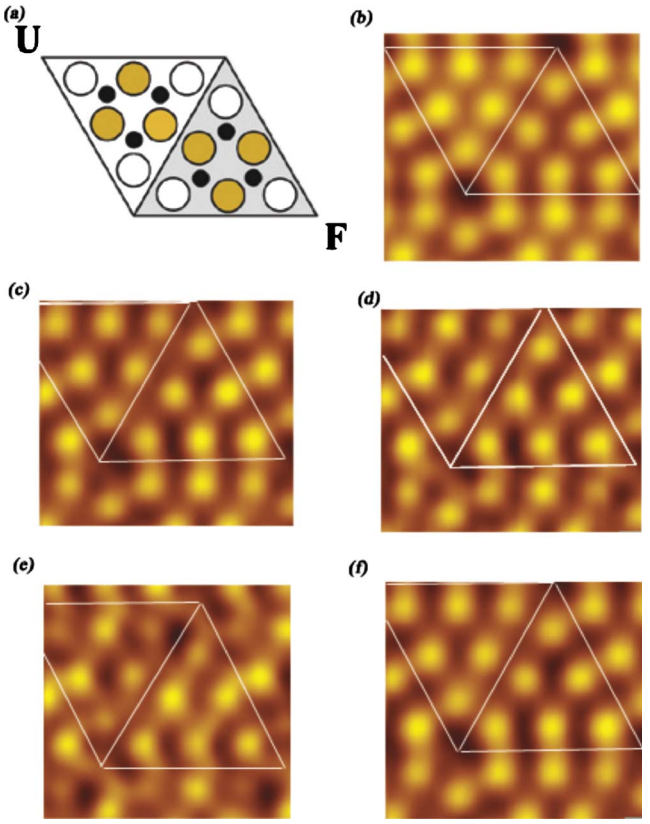

FIG. 1. (Color online) DAS model of Si(111)−7×7 surface and STM topographic images. (a) Schematic illustration of a unit cell is based on the DAS model of Si(111)−7×7, where the open circles, filled-yellow circles, and black dots represent corner adatoms, center adatoms, and rest atoms, respectively. These are the surface atoms with dangling bonds. The short diagonal divides the unit cell into the unfaulted half cell (U) and the faulted half cell (F). The empty state topographic image is obtained at 4.3 K by using a UHV STM system with a cleaned Pt-Ir tip for a tip height defined by setting the tunneling current (I_s) to (b) 10 pA, (c) 200 pA, (d) 400 pA, (e) 500 pA, and (f) 100 pA after the scan at 500 pA. For all images, a unit cell and its short diagonal are marked with white lines. It shows that the approximate symmetry between the unfaulted and the faulted half cells diminishes as the tip height reduces. Note that the rest atoms do not appear in empty-state images and the long diagonal of a unit cell is about 5 nm.

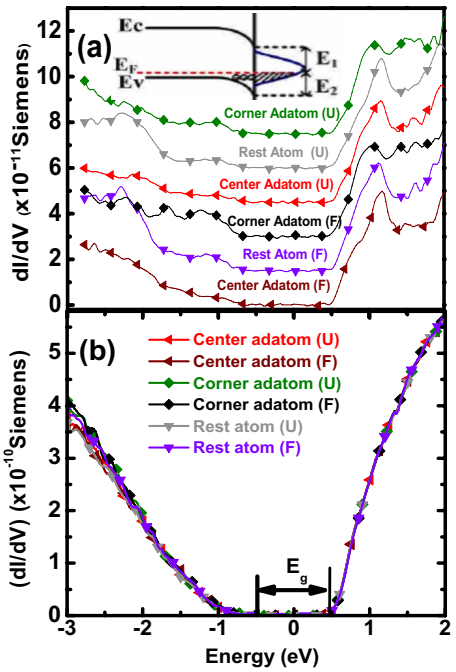

FIG. 2. (Color online) Spectra of differential conductance measured at the six atomic sites along the long diagonal of a unit cell at 4.3 K. (a) Spectra taken at tip height defined by I_S=50 pA indicate that each atom has its own features despite the common energy gap. The positive gap edge is similar to the bulk conduction-band edge E_c=0.52 eV relative to the chemical potential, shown in the inset. However, the negative gap edge is less well defined and has a value about 0.9 eV, which is larger than the valence-band edge E_v =0.65 eV. Additional band bending due to reverse bias may be the reason for the discrepancy. (b) Spectra taken at a lower tip height defined by I_S=500 pA show convergence at all atomic sites. The common empty-state spectrum (at positive bias) resembles the bulk DOS, i.e., $\propto\sqrt{E-E_C}$. The notation E_g denotes the magnitude of bulk Si semiconductor gap.

T=4.3 K (Fig. 1). A standard empty-state image, being symmetric with respect to the short diagonal, is obtained with a relatively large tip height defined by a setting current I_s =10 pA [Fig. 1(b)]. The "brightness" of all adatoms appears equal. The topographic images of the same surface become increasingly asymmetrical across the short diagonal as the tip height is lowered, which are shown in Figs. 1(b)–1(e). In the image of I_s=500 pA [Fig. 1(e)], the adatoms in the faulted half are brighter than those in the unfaulted half. Furthermore, the image of the unit cell returns to its pristine form as the tip is elevated back to a higher position [Fig. 1(f)]. This proves that the change of contrast cannot be due to any permanent movement of the surface atoms. According to the DAS model, the two halves differ from each other only in the third layer of atoms. Thus this change of image contrast inspired us to study the DOS as the tip height reduces. To elucidate the evolution of the DOS, we measure the $I(V)$ curves at six atomic sites along the long diagonal of the unit cell and at different tip heights set by I_s. Figure 2(a) shows the spectra (dI/dV) at a tip height of I_s=50 pA. The spectra are increasingly shifted vertically for clarity and they demonstrate the individual spectral features of each atom. However, a gap close to the Si bulk gap is evident in all spectra. Most surprisingly, the spectra of I_s=500 pA fall into a single curve at all atomic sites [Fig. 2(b)]. This common empty-state spectrum remarkably resembles the bulk DOS, i.e., $\propto\sqrt{E-E_C}$, with E_C=0.52 eV relative to the bulk chemical potential. It is in stark contrast to the expected result for a metallic surface.

We further reveal the effect of bulk electronic states on tunneling spectrum by showing the normalized spectra $(dI/dV)/(I/V)_{average}$ of the surface-atom sites in the faulted half cell at 4.3 K for three different tip heights (Fig. 3). The spectra for the unfaulted-half cell are not shown because the respective atoms in the both faulted-half and unfaulted-half cells have similar spectral features except different peak heights. The $(I/V)_{average}$ is calculated according to Eq. (1), a scheme proposed by Mårtensson and Feenstra,[18]

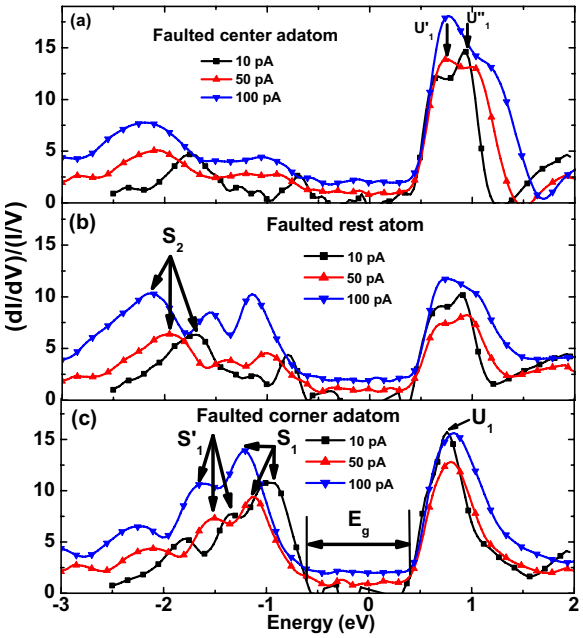

FIG. 3. (Color online) $(dI/dV)/(I/V)_{average}$ spectra at atom sites in the faulted half cell obtained with decreasing tip heights at 4.3 K. The spectra are measured by I_S=10, 50, and 100 pA at (a) center adatom, (b) rest atom, and (c) corner adatom sites. In addition to the surface states identified in the spectra at 20 K, the spectra at 4.3 K possess an extra feature of energy gap. This energy gap is attributed to the bulk Si semiconductor gap, as shown in our numerical calculation. The parameters of a and ΔV in $(I/V)_{average}$ are 2 and 1.3, respectively. The value of energy state is insensitive to the choice of these two parameters. For clarity, the spectra are shifted vertically.

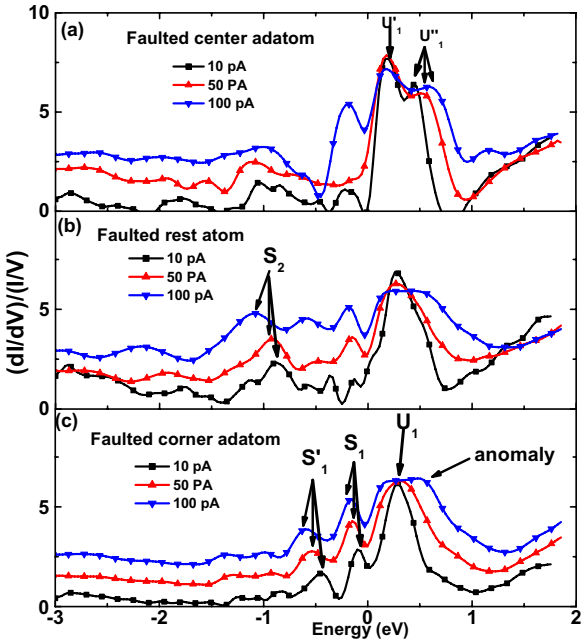

FIG. 4. (Color online) $(dI/dV)/(I/V)_{average}$ spectra at atom sites in the faulted half cell obtained with decreasing tip heights at 20 K. The spectra are measured by I_S=10, 50, and 100 pA at (a) center adatom, (b) rest atom, and (c) corner adatom sites. The bulklike gap is absent in the spectra at 20 K, in agreement with the theoretical prediction for a metallic surface. However, the current-dependent energy shifts of the surface-state features are evident. Arrows indicate the respective surface states. The same parameters of a and ΔV with Fig. 3 are used. For clarity, the spectra are shifted vertically.

$$(I/V)_{average} = \frac{1}{2\Delta V} e^{a|V|} \int_{-\infty}^{\infty} \frac{I_S(V')}{V'} e^{-|V'-V|/\Delta V} e^{-a|V'|} dV'. \quad (1)$$

The normalization by $(I/V)_{average}$ reduces the influence of the tip-sample separation set by I_s and removes the divergence of normalized differential conductance $(dI/dV)/(I/V)$ in the regime of very low tunneling currents. Some surface states are evident, but their energy positions are clearly up shifted by an apparent gap. To understand the origin of the energy shift, we repeat the same measurements at a higher temperature, T=20 K, and the results are in Fig. 4. Now the surface states corresponding to center adatom (U_1', U_1''), rest atom (S_2), and corner adatom $(S_1'$, S_1, and $U_1)$ can be clearly identified (Fig. 4). The spectra at 20 K clearly display the gapless states, indicative of a metallic surface. However, even without the gap in the spectra, the surface-state features still shift up in energy with lowering tip height. In comparison to the spectra at 20 K, we tentatively assigned the surface states as shown in Fig. 3.

We summarize the dependence of energy values of surface states on I_s at 20 and 4.3 K in Fig. 5. The energy values of all six states are linearly dependent with I_s for both temperatures. By extrapolating the energy of each state to zero I_s, we can obtain the unperturbed energy positions of these surface states. At 20 K, the energy values of states S_2, S_1', S_1, U_1', U_1, and U_1'' are −0.84, −0.44, −0.08, 0.17, 0.29, and 0.42 eV respectively, while they are −1.66, −1.35, −0.95, 0.64, 0.75, and 0.92 eV, respectively, at 4.3 K. Since there is no energy deviation in the values obtained at 20 K, we suppose that these values at 20 K represent the correct energy values of the surface states.[19] In Fig. 6, we show the extrapolation energy values of the surface states at 20 and 4.3 K. Interestingly, the energy difference between the empty states at 20 and 4.3 K is about 0.5 eV, close to the conduction-band edge of bulk Si [inset of Fig. 2(a)]. The corresponding difference in the filled states is about 0.9 eV, which is larger than the expected 0.65 eV of the bulk valence-band edge suggested by surface band bending.[20] This larger shift and deviation from the typical form of semiconductor energy gap may be attributed to the enlargement of the Schottky barrier in the reverse bias. Despite the absence of a bulklike gap in the spectra of 20 K, the influence of bulk states likely causes the deformation around 0.5 eV in the spectrum of I_s=100 pA. The effects of both temperature and current on the energy shift of the surface states strongly suggest that the chemical potential of the surface states is deviated from the chemical potential of the substrate.

To understand the evolution with tip height clearly, we measured the tip-height dependence of tunneling current at different sites (Fig. 7). If the tunneling resistance is dominated by a vacuum barrier[14]

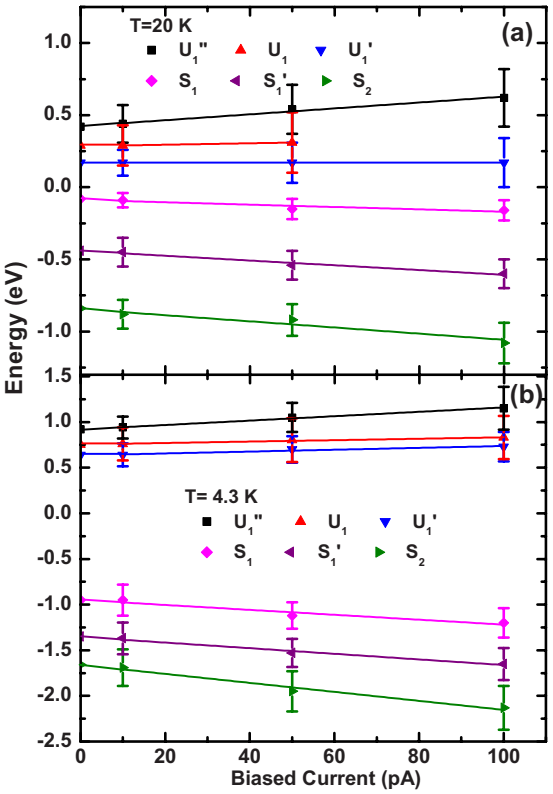

FIG. 5. (Color online) Current dependence of energy shift of surface states. Data points are obtained from Figs. 4 and 3 at (a) 20 K and (b) 4.3 K, respectively. Lines are drawn according to linear fits. The error bars are estimated by respective spectral widths. By extrapolating the energy of each state to zero I_s, we can obtain the energy values of states S_2, S_1', S_1, U_1', U_1, and U_1'' at 20 K are −0.84, −0.44, −0.08, 0.17, 0.29, and 0.42 eV respectively, while they are −1.66, −1.35, −0.95, 0.64, 0.75, and 0.92 eV, respectively, at 4.3 K. This figure shows that the major difference between the spectra at 20 and 4.3 K is the extra energy gap presented in the spectra at 4.3 K. Based on our model, this is the bulk Si semiconductor gap.

$$\phi_A(\mathrm{eV}) = 0.952\left(\frac{d\ln I}{dz(\text{Å})}\right)^2, \tag{2}$$

all data points should fall on a universal line in this $I(z)$ plot. Indeed, this is the case for a span of 0.2 nm near $z=0$ defined by $I_s=10$ pA. A barrier ϕ_A of 2.8 eV is thus derived, which is close to the value of 3.1 eV reported on a p-type Si substrate.[21] However, $I(z)$ becomes site dependent for z less than −0.1 nm. Since the difference in $I(z)$ is insignificant between the corresponding atoms in the two halves, we focus our discussion on the unfaulted half [Fig. 7(a)]. The slope of $\ln[I(z)]$ decreases monotonically below $z=-0.1$ nm at the rest atom site. At the adatom sites, there is a deviation in the range of $z=-0.15$ to −0.2 nm, where the tunneling current for the center adatom site increases more rapidly. A similar phenomenon has been observed as the tip approaches some metal surface, which has been attributed to the tip-surface relaxation.[15–17] No relaxation is observed at the corner adatom, suggesting that its bonding with substrate atoms is stronger. In fact, we have observed that the center adatom can be displaced by high tunneling currents at temperatures

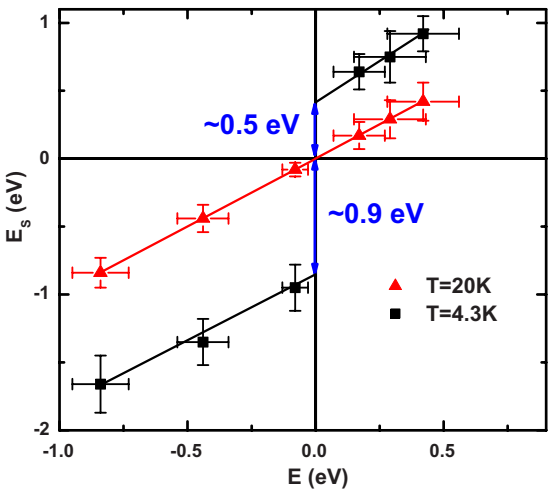

FIG. 6. (Color online) Correspondence between the measured energy values and correct energy values of the surface states at 20 and 4.3 K. We suppose that the energy value obtained at 20 K is the correct surface-state energy. The correct surface-state energy is shown in the x axis and the measured energy value is shown in the y axis. This figure shows that the energy positions at 4.3 K are shifted from the respective ones at 20 K by about 0.5 and 0.9 eV in the positive and negative biases, respectively. Error bars are estimated from the spectral widths of respective states.

higher than 10 K, while no displacement of the corner adatom is induced under the same condition. The previous report of manipulation of Si center adatoms is consistent with our result.[22] Below $z=-0.2$ nm, the apparent barrier heights at both adatom sites reduce to 0.2 eV or less, indicative of tunneling-barrier collapse. Thus we conclude that the overlapping of the electron wave functions between the tip and the surface is significantly enhanced at $I_s=500$ pA($z=-0.23$ nm), but not enough to push the surface atoms out of their equilibrium positions. The fact that the magnitude of ϕ_A reduction is different at different sites and yet $I(V)$ becomes universal at $I_s=500$ pA strongly suggests that the mechanism is not due to surface or tip atom alterations, multiple tunneling-scattering effect, or any other effect involving only the tip and the surface layer.

The inhomogeneous ϕ_A in the regime of high tunneling current could be attributed to interactions between the tip atom and surface atoms. Hofer and Fisher found that tunneling conductance is proportional to the tip-surface interaction energy.[23] They proposed that the current flow between individual atoms is a measure for their interaction. Since the dangling bonds of the three atoms have different filling factors,[2] the interactions with the tip atom would vary at the three atom sites. Therefore, the $I(z)$ curves behave differently.

The above discussion leads us to contemplate the possibility that the chemical potential of bulk electrons (μ_B) and surface electrons (μ_S) may actually be separated from each other by the tunneling current. The dangling bonds on the 7×7 surface usually enable the pinning of μ_B and μ_S, which results in band bending as illustrated in the inset of Fig. 2(a). If the bulk-surface coupling is so strong that the two levels are tied together even at high current, then the tunneling

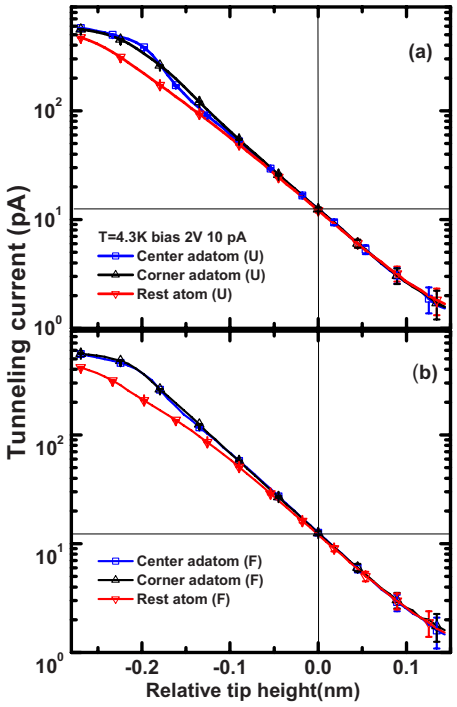

FIG. 7. (Color online) $I(z)$ curves of the center adatom, corner adatom, and rest atom. The $I(z)$ curves of these atoms in the unfaulted half cell are shown in (a) and the respective data in the faulted half cell are shown in (b). The current is measured with a fixed sample bias voltage of +2 V at 4.3 K. The zero point of z is arbitrarily chosen to be the tip height defined by I_S=10 pA at all six atomic sites along the long diagonal of a unit cell. Smaller value of z represents closer tip to surface separation. For each set of I-vs-z measurement, after releasing the z-control feedback with I_S =10 pA(z=0), the tip is first retracted back by about 0.2 nm. Then the z dependence of the tunneling current is measured by pushing the tip toward the surface in 50 steps. For clarity, only a small number of the 50 data points are shown as the individual symbols on the line which is fitted through the entire data set. The error bar on the symbol is determined by the noise of our current amplifier. A barrier ϕ_A of 2.8 eV is derived.

spectrum should always reveal the surface DOS with or without the influence of the bulk wave functions. A separate measurement of the tip-surface contact current, with a fixed bias at +2 V in the temperature range between 4 and 20 K, shows a thermally activated resistance with an activation energy of 4 meV. Thus it is plausible that the large resistance of tunneling current through the bulk at low temperatures causes the detachment of μ_S from μ_B. Under the influence of current, μ_S moves between μ_B and the tip chemical potential μ_T. The difference of the latter two is the biased voltage. This scenario naturally leads to up-shifting of the surface features of the tunneling spectra with increasing I_s. More importantly, it can explain the universally bulklike $I(V)$ curve when I_s is 500 pA at 4.3 K if we surmise that μ_S is nearly pinned to μ_T at that point as implied by observed vacuum barrier collapse. In this situation, the tunneling spectrum is determined by the product of the mixed DOS combining surface and tip states to the bulk states. Thus the gapped bulk DOS dominates the $I(V)$ curve. This model of surface chemical-potential shifting is consistent with the theoretical study showing that the current flow between individual atoms is a measure of their interaction strength.[23]

IV. NUMERICAL MODEL

In our numerical calculation, the potential is set to be zero at the chemical potential of the bulk electrons (μ_B). The external voltage bias is then equal to the chemical potential of the tip electrons (μ_T) divided by the electron charge e. For simplicity, we further assume that the DOS of the tip is a constant in the bias range of 2 V. Ignoring thermal excitation, the tunneling current, I_1, between the tip and the surface states can be approximately written as the following equation:

$$I_1 = A\int_{\mu_S}^{eV} \rho_s(\varepsilon - \mu_S)T(\varepsilon, eV)d\varepsilon. \tag{3}$$

Here, $T(\varepsilon, eV)$ is the tunneling matrix element, μ_S is the chemical potential of the surface electrons (or expressed as eV_2), and ρ_s is the density of the silicon surface states. The current, I_2, between the surface and bulk states, is assumed to take the tunneling form because of the relatively weak coupling between the two states

$$I_2 = \int_0^{\mu_S} \left[C\left(\mathrm{Re}\sqrt{\frac{\varepsilon}{E_C} - 1} \right) + D\frac{\gamma^2}{\pi(\varepsilon^2 + \gamma^2)} \right] \times \rho_s(\varepsilon - \mu_S)T(\varepsilon, \mu_S)d\varepsilon, \tag{4}$$

where the density of the bulk states is modeled by a gapped DOS with a conduction-band edge at E_C=0.52 eV and a density of dopant states of Lorentzian form with an energy width of γ=0.1 eV. We also assume that the functional form of $T(\varepsilon, eV)$ is similar in both tip-to-surface and surface to bulk tunnelings. Although the spectrum of $(dI/dV)/(I/V)_{average}$ is proportional to DOS, the tunneling matrix element still contains an exponential factor of voltage bias according to the WKB approximation.[2] It is better to choose $\rho_s(\varepsilon - \mu_S)T(\varepsilon, eV)$ to be the measured $(dI/dV)/(I/V)_{1.85\ \mathrm{V}}$ of the specified tunneling site at 20 K at the tip height fixed by I_s=10 pA. The reason why we divided dI/dV by $(I/V)_{1.85\ \mathrm{V}}$ is to let the unit of $\rho_s(\varepsilon - \mu_S)T(\varepsilon, eV)$ become dimensionless and choosing 1.85V is arbitrary as long as I/V is not too small.

The constants A, C, and D are fitting parameters to be determined. The continuity of current requires the equality of I_1 and I_2. Solving this equation, I_1=I_2, gives us the value of μ_S in terms of the three fitting parameters. Thus we obtain the $I(V)$ curve in the chosen range of the external biased voltage V. The value of A dictates the strength of the tip-surface coupling. Therefore, it should become larger when the tip is closer to the surface. Meanwhile, the strength of the surface-bulk coupling near the Fermi level is related to the value of D. We first determine these three values at 4.3 K and I_s=10 pA. From Eq. (4), we know that the value of D dominates the tunneling current in voltage range from 0 to 0.52 eV. Because the measured tunneling current in this range is down to the noise level, we can only determine an upper

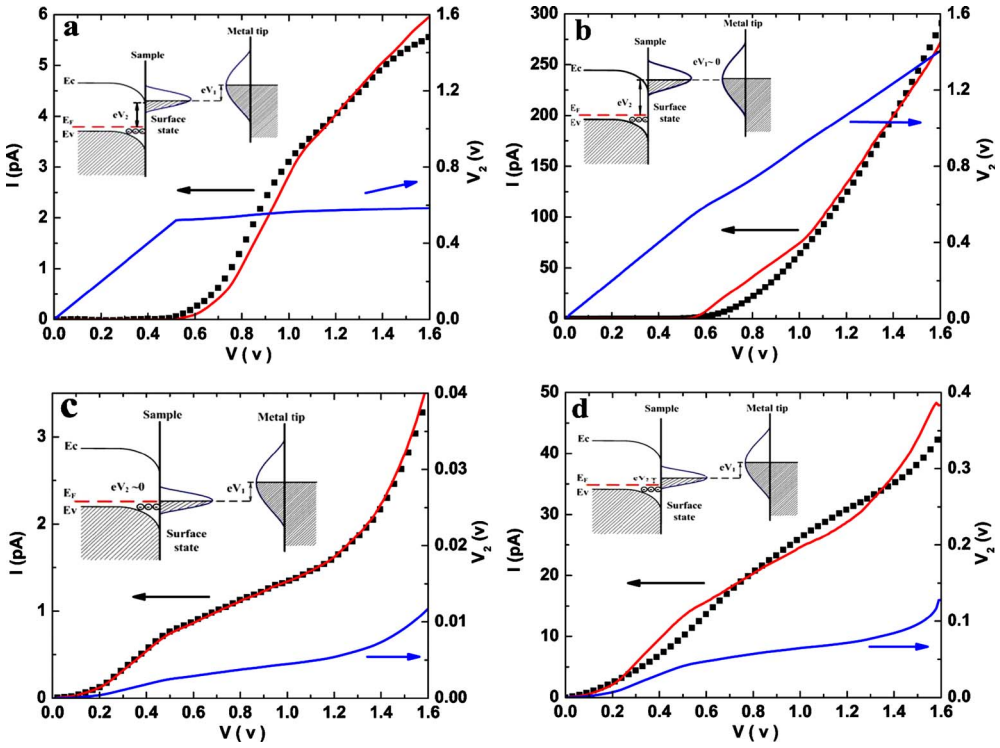

FIG. 8. (Color online) Simulated results and experimental data of *I-V* curve. Insets are the schematic illustrations of relative chemical-potential positions in respective modeling situations. Black dots are experimental data, red line is the simulated result, and blue line (V_2), referred to the right axis, is the shift of μ_S relative to μ_B. At 4.3 K, the values of A, C, and D are (a) 1.53×10^{-11}, 3×10^{-9}, and 3×10^{-12} A/eV, respectively, for I_S=10 pA, and (b) 7.7×10^{-9}, 3×10^{-9}, and 3×10^{-12} A/eV, respectively, for I_S=500 pA. At 20 K, the values of A, C, and D are (c) 3.9×10^{-12}, 3×10^{-9}, and 9×10^{-9} A/eV, respectively, for I_S=10 pA, and 6.7×10^{-10}, 3×10^{-9}, and 9×10^{-9} A/eV, respectively, for I_S=100 pA (d).

bound of D which we choose for all fittings at 4.3 K. Then we choose a fixed point in our experimental data and demand all calculated *I-V* curves to go through this point. Through this fixed-point procedure, the parameters A and C are no longer independent. By changing C, we can have different sets of A, C, and D. The set that can fit the experimental data best in the entire range of V is the best fitting parameters. The coupling strength does not vary with different setting current, so the values of C and D should remain unchanged at the same temperature. Because of this reason, we just need to change A to fit the fixed point in the case of I_s=500 pA. At 20 K, we also work on I_s=10 pA first. Since the value of C indicates the contribution of Si conduction band to the tunneling current, it should be insensitive to temperature. Therefore, the value of C at 20 K is chosen to be the same as that at 4.3 K. The method we use to find the remaining A and D is the same as that we find A and C at 4.3 K. Through fitting the *I-V* curves at 4.3 K, we obtain a fixed value of C and setting current-dependent A with a negligible D. Then with the same fixed C, we again obtain a fixed value of D and values of A which are dependent on the setting current through fitting *I-V* curve at 20 K.

Figure 8 shows a series of raw data and simulated results at faulted corner adatom site at 4.3 and 20 K. The left axis is referred to current and the right axis is referred to voltage (V_2) indicating the relative shift of μ_S to μ_B at different external biased voltages. According to the simulated result of μ_S, we schematically illustrate the modeling situation of tunneling in the respective inset of the subfigure. At 4.3 K, the small value of D leads to a negligible current below the minimum of conduction-band edge and thus V_2 is equal to V. The increase of biased current, thus the value of A, farther shifts μ_S to μ_T, which is shown in the evolution of μ_S curves from Fig. 8(a) (I_s=10 pA) to Fig. 8(b) (I_s=500 pA). For small I_s such as 10 pA, μ_S is raised to the conduction-band edge and keeps to this energy value so that observed tunneling spectra reveal shifted surface states. On the other hand, for large I_s such as 500 pA, μ_S is nearly leveled to μ_T. There is hardly a voltage drop between the chemical potentials of the tip (μ_T) and the surface states (μ_S) so that a universal bulk DOS is revealed in the spectra of STS. This is consistent with the results of $I(z)$ indicating the collapsed barrier of vacuum tunneling at 500 pA (Fig. 7).

At 20 K, the coupling strength (D) of surface states to the dopant band is stronger, which is 10^3 times larger than the coupling strength at 4.3 K. For low setting currents at 20 K, μ_S is practically pinned to the dopant level μ_B. In Fig. 8(c) (I_s=10 pA), current appears in the gap region of bulk Si and the value of V_2 is negligible small. Thus the observed spectra show the typical surface states. The larger voltage shift observed at I_s=100 pA, shown in Fig. 8(d), can explain the deformation around 0.5 eV in the spectra of I_s=100 pA in Figs. 4(b) and 4(c). The simulation not only quantitatively explains the experimental data but also accounts for the constant energy difference of 0.5 eV between the empty surface states at 4.3 and 20 K as well. The energy shift of surface

states due to the semiconductor gap is eliminated by increasing the value of D, thus enhancing the surface-bulk coupling. The good agreement between the simulations and data suggests that we have unraveled the interfacial coupling between the surface states and the bulk states. In Fig. 1(e), which is scanned as vacuum tunneling barrier collapses, the image contrast in addition to the arrangement of the surface atoms could be attributed to the different surface to bulk conductivity in the two half cells. The surface to bulk conductivity in the faulted half cell is higher than that in the unfaulted half cell, thus the faulted half appears brighter in Fig. 1(e). Theoretical study of the surface to bulk conduction in the system of the Si(111)-7×7 surface is needed to compare with our experimental data.

V. CONCLUSION

Using a UHV low-temperature STM system, we have observed the evolution of topography on the Si(111)-7×7 surface with decreasing STM tip height at $T=4.3$ K. Our result shows a sharper contrast between the faulted and unfaulted halves of the 7×7 unit cell as the tip is closer to the surface. Since the surface layers of adatoms and rest atoms in the two halves are symmetrical, this contrast implies that the tunneling tip can sense the subsurface layer. Furthermore, the tunneling spectra taken at individual atomic sites also evolve from $I(V)$ curves showing features characterizing individual atoms to a universal $I(V)$ curve resembling the bulk silicon gap. At 20 K, this energy gap disappears and surface states of Si atoms are observed at all tip heights used. However, the surface features do shift up in energy as the tip becomes closer to the surface. To reveal the underline mechanism of these evolutions, the tip-height dependence of tunneling current for different atomic site is measured at 4.3 K. The result shows that apparent barrier heights (ϕ_A) of the surface atoms correspond to a universal value, typical of vacuum tunneling, at relative large tip-surface separation and become inhomogeneous showing different degree of tunneling-barrier collapse. Only the center adatoms show the evidence of the tip-surface relaxation. Thus the fact that all tunneling $I(V)$ curves, taken at the smallest separation, become universal cannot be explained by the mechanism of the tip-surface relaxation, the multiple tunneling effect, or any other effect related to individual surface atoms.

In order to explain the observed phenomena, we have developed a model allowing the surface chemical potential to be shifted away from that of the bulk state due to high tunneling currents. Normally, the surface chemical potential is pinned to that of the bulk, thus the surface density of state is obtained by ramping the tunneling potential difference between the tip and the surface in tunneling experiment. However, in the extreme case when the surface chemical potential is shifted and pinned to that of the tip, then it would be natural to observe the bulklike tunneling $I(V)$ curve. In order to show this simple model can quantitatively explain the $I(V)$ curves, we have performed numerical calculations for various tip heights defined by the setting currents. With only three fitting parameters, the simulated I-V curves are in reasonably good agreement with the measured ones. By virtue of the good fitting, we can obtain the relative coupling strength of between surface states and the bulk states with atomic resolution. We believe this is a methodology to explore the subsurfaces of Si and can be applied to other interesting materials as well.

ACKNOWLEDGMENT

This work is supported by the NSC under Project No. NSC98-2120-M-007-005.

[1] G. Binnig, H. Rohrer, C. Gerber, and E. Weibel, Phys. Rev. Lett. **49**, 57 (1982).
[2] C. J. Chen, *Introduction to Scanning Tunneling Microscopy*, 2nd ed. (Oxford University Press, New York, 2008).
[3] S. H. Pan, J. P. O'Neal, R. L. Badzey, C. Chamon, H. Ding, J. R. Engelbrecht, Z. Wang, H. Eisaki, S. Uchida, A. K. Gupta, K.-W. Ng, E. W. Hudson, K. M. Lang, and J. C. Davis, Nature (London) **413**, 282 (2001).
[4] G. A. Fiete and E. J. Heller, Rev. Mod. Phys. **75**, 933 (2003).
[5] I. Matsuda, M. Ueno, T. Hirahara, R. Hobara, H. Morikawa, C. Liu, and S. Hasegawa, Phys. Rev. Lett. **93**, 236801 (2004).
[6] F. Meier, L. Zhou, J. Wiebe, and R. Wiesendanger, Science **320**, 82 (2008).
[7] W. J. Kaiser and L. D. Bell, Phys. Rev. Lett. **60**, 1406 (1988).
[8] A. Ohtomo and H. Y. Hwang, Nature (London) **427**, 423 (2004).
[9] S. Thiel, G. Hammerl, A. Schmehl, C. W. Schneider, and J. Mannhart, Science **313**, 1942 (2006).
[10] C. Cen, S. Thiel, G. Hammerl, C. W. Schneider, K. E. Andersen, C. S. Hellberg, J. Mannhart, and J. Levy, Nature Mater. **7**, 298 (2008).
[11] K. Takayanagi, Y. Tanishiro, M. Takahashi, and S. Takahashi, J. Vac. Sci. Technol. A **3**, 1502 (1985).
[12] R. Schillinger, C. Bromberger, H. J. Jänsch, H. Kleine, O. Kühlert, C. Weindel, and D. Fick, Phys. Rev. B **72**, 115314 (2005).
[13] T. Tanikawa, K. Yoo, I. Matsuda, S. Hasegawa, and Y. Hasegawa, Phys. Rev. B **68**, 113303 (2003).
[14] N. D. Lang, Phys. Rev. B **37**, 10395 (1988).
[15] L. Olesen, M. Brandbyge, M. R. Sorensen, K. W. Jacobsen, E. Laegsgaard, I. Stensgaard, and F. Besenbacher, Phys. Rev. Lett. **76**, 1485 (1996).
[16] W. A. Hofer, A. J. Fisher, R. A. Wolkow, and P. Grütter, Phys. Rev. Lett. **87**, 236104 (2001).
[17] Y. Sun, H. Mortensen, S. Schär, A. S. Lucier, Y. Miyahara, P. Grütter, and W. Hofer, Phys. Rev. B **71**, 193407 (2005).
[18] P. Mårtensson and R. M. Feenstra, Phys. Rev. B **39**, 7744 (1989).
[19] J. Mysliveček, A. Stróżecka, J. Steffl, P. Sobotík, I. Ošt'ádal, and B. Voigtländer, Phys. Rev. B **73**, 161302(R) (2006). The energy values for these surface states are rather close to or slightly smaller than those reported in this paper, except for S_2 for which our value is 8% larger.

[20] G. Hollinger and F. Himpsel, J. Vac. Sci. Technol. A **1**, 640 (1983).
[21] S. Kurokawa, M. Yuasa, A. Sakai, and Y. Hasegawa, Jpn. J. Appl. Phys. **36**, 3860 (1997).
[22] B. C. Stipe, M. A. Rezaei, and W. Ho, Phys. Rev. Lett. **79**, 4397 (1997).
[23] W. A. Hofer and A. J. Fisher, Phys. Rev. Lett. **91**, 036803 (2003).